Nr 3 (133–192) MARZEC 2023 Tom LXVIII

POLIMERY

EVA/zinc oxide nanocomposites for active food packaging: selected physical, and microbial properties

Haza Satar Majeed[1), *)] (ORCID ID: 0000-0002-2293-9583), **Farah Khalaf Hammoud Al-Juboory**[2)] (0000-0002-3845-226X), **Raghad Ali Hamid**[1), 3)] (0000-0003-1156-1586), **Ruzniza Mohd Zawawi**[3)] (0000-0003-1714-9605)

DOI: https://doi.org/10.14314/polimery.2022.6.1

Abstract: The melt-mixing method was used to obtain nanocomposites of poly(ethylene-co-vinyl acetate) (EVA) with 1, 3 or 5 wt% of hydrophilic zinc oxide (ZnO) nanoparticles. The contact angle, barrier and antimicrobial properties of the obtained composites were investigated. The nanocomposites were characterized by better hydrophilic and barrier properties, as evidenced by, respectively, a smaller contact angle and lower water vapor permeability and water absorption compared to EVA, which can be explained by the formation of hydrogen bonds between EVA and ZnO. In addition, the composites were characterized by greater bactericidal activity against *E. coli* and *S. aureus*. The optimal physical and microbial properties were obtained with 3 wt% ZnO content.

Keywords: ZnO nanoparticles, ethylene vinyl acetate copolymer, barrier properties.

Nanokompozyty EVA/tlenek cynku do aktywnych opakowań do żywności: wybrane właściwości fizyczne i mikrobiologiczne

Streszczenie: Metodą mieszania w stanie stopionym otrzymano nanokompozyty kopolimeru etylen-octan winylu (EVA) z dodatkiem 1, 3 lub 5%mas. hydrofilowych nanocząstek tlenku cynku (ZnO). Zbadano kąt zwilżania, właściwości barierowe i przeciwdrobnoustrojowe otrzymanych kompozytów. Nanokompozyty charakteryzowały się lepszymi właściwości hydrofilowymi i barierowymi, o czym świadczy, odpowiednio, mniejszy kąt zwilżania oraz mniejsza przepuszczalność pary wodnej i absorpcja wody w porównaniu z EVA, co można wyjaśnić tworzeniem się wiązań wodorowych pomiędzy EVA i ZnO. Ponadto kompozyty miały większą aktywność bakteriobójczą wobec *E. coli* i *S. aureus*. Optymalny zespół właściwości uzyskano przy 3% mas. zawartości ZnO.

Słowa kluczowe: nanocząstki ZnO, kopolimer etylen-octan winylu, właściwości barierowe.

Microbial contamination is a major problem in food packaging, storage, and transportation. It further decreased the quality and shelf lives of the foods [1]. Smart packaging protects against both external and internal factors [2]. An introduction of antimicrobial compounds in the packaging films can inhibit the microbial growth and increase the shelf-lives of the food products [3]. In this process, the packaging films were coated with many antimicrobial compounds which can kill or inhibit the growth of microbes on the food surfaces. It also increases the functional properties of the packaging

[1)] Department of Chemistry, College of Education for pure science, University of Kirkuk, Iraq.

[2)] Kirkuk university/College of science/chemistry department.

[3)] Department of Chemistry, Faculty of Science, University Putra Malaysia, Serdang 43400, Malaysia.

[*)] Author for correspondence: hazasatarmajeed@gmail.com

materials by decreasing the growth of the microorganisms and increasing the shelf life of all products [3].

Poly(ethylene-co-vinyl acetate) (EVA) copolymer was commonly used for packaging food products. EVA combined the material and chemical properties of the chemically-cross-linked elastomeric compound with the engineered sticks that were cost-effective and easily manufactured. This polymer is an elastic material which is sintered for forming a porous product, like rubber, with high toughness [4]. Researchers stated that EVA could be used as an effective polymer in many applications like food packaging, pharmaceuticals, and development of medical devices. It was an innovative material which could be tailored for developing many novel products that could be used for different applications [5, 6].

The EVA nanocomposites were a novel class of nanoparticles which included the properties of nanofillers, engineered sticks, nanofillers and elastomers. The small size of the nanoparticles could affect the EVA properties and significantly enhance their mechanical and physical performance [7, 8]. George *et al.* [9] developed EVA/graphite nanocomposites using commercially expanded and tailor-made graphite nano-flakes. The dynamic and static mechanical properties of the composites were significantly improved compared to pure polymers. Some researchers studied the biomedical properties of silver/titanium dioxide (Ag/TiO2) incorporated LDPE/EVA nanocomposites. They noted that the silver nanoparticles were uniformly dispersed on TiO_2 nanoparticles in LDPE/EVA blend, which enhanced the antimicrobial properties of the films [10]. The incorporation of inorganic nanoparticles was seen to be an effective strategy which improved the properties of the polymeric materials. The zinc oxide (ZnO) nanostructures showed a larger volume to area ratio, good mechanical properties, a crystalline structure, higher thermal conductivity and a lower coefficient of thermal expansion. Hence, they were regarded to be potential candidates that could be used as a reinforcing filler material in the polymer composites. They also showed a higher radiation hardness, good antimicrobial activities and high ultraviolet absorption, when the solution pH ranged between 7 and 8. As a result, they could be used in various applications like gas sensors [11], catalysts [12], antimicrobial compounds [13] and optical devices [14].

Many researchers have used ZnO-based polymer nanocomposites in different applications; however, very few used EVA films for food packaging applications. This study presents the effect of ZnO nanoparticles on EVA selected physical, barrier and antimicrobial properties.

EXPERIMENTAL PART

Materials

Poly(ethylene-co-vinyl acetate) (EVA) with the trade name Ube Polyethylene V215 (Ube-Maruzen Polyethylene Co. Ltd., Japan) was supplied by Zarm Scientific and Supplies, Sdn. Bhd. EVA contained 15wt% of vinyl acetate and 85wt% of ethylene. ZnO nanoparticles and magnesium nitrate-6-hydrate were supplied from Sigma-Aldrich Chemical Co. (USA).

Methods

Fourier infrared spectroscopy

Fourier infrared spectroscopy (FTIR) (Perkin Elmer, model Spectrum 100, USA) was used to analyze the chemical structure. The spectra were recorded using at least 64 scans with 4 cm^{-1} resolution, in the spectral range of 4000–300 cm^{-1}, using powder samples (63 μm).

X-ray diffraction

X-ray diffraction (XRD) was used to study the composites crystalline phase. The samples were analyzed using a Shimadzu model XRD-6000 diffractometer using Cu-Kα radiation at 30 kV and 30 mA, which is generated by a Philips 2.7 Kw wide focus X-ray diffraction tube. The analysis was performed at ambient temperature and was performed at 2θ in the range of 5° to 80° with a scan rate of 2°/min. The sample was removed and then placed on an aluminum sample holder. In XRD, a collimated X-ray beam of λ ~ 1.54 Å was incident on the sample and diffracted over the crystalline phase in the sample according to Bragg's law (Eq. 1).

$$N\lambda = 2\,d\,\sin\theta \qquad (1)$$

where: N – the integer (number of peak), λ – the wavelength of incident wave, d – the spacing between the planes in the atomic lattice/lattice spacing, θ – the angle between the incident ray and the scattering planes.

The results were compared with the Joint Committee on Powder Diffraction Standard (JCPDS) and generated graphs of diffraction peaks were used to calculate the crystalline phase.

Thermogravimetric analysis

Thermogravimetric analysis (TGA) was performed using thermogravimetric analyzer (TGA/SDTA 851, Mettler Toledo, USA) in nitrogen atmosphere at heating rate of 10°C/min, from 25 to 700°C.

Water contact angle (WCA)

The hydrophobicity of EVA/ZnO nanocomposites was determined by measuring the water contact angle (WCA) using the Theta Lite tensiometer (Biolin Scientific, Sweden). A sessile drop process was applied. The water contact angle was measured at 5 locations on the sample surface, and the WCA value was the average for five measurements.

Water absorption (WA)

The samples were dried in a desiccator for 1 week at 0% relative humidity. They were then placed in another container at 100% relative humidity and allowed to absorb water to constant weight. The water uptake of the samples was calculated using the following formula:

$$\text{Water uptake} = [(W_f - W_i)/W_i] \times 100 \quad (3)$$

W_i and W_f were the initial and final (equilibrium) weights of the samples, respectively. The average of five measurements was taken as the result.

Water vapour permeability (WVP)

Water vapor permeability (WVP) was measured at 25°C according to ASTM E96-95 standard gravimetric method using 3.5 cm diameter Payne permeability cups. The samples were equilibrated at 54% relative humidity with magnesium nitrate 6-hydrate. The WVP for the samples was estimated using the following formula:

$$WVP = (\Delta m \times l)/ (A \times t \times \Delta P) \quad (4)$$

wherein, Δm – the weight loss noted in every cup; l – film thickness; A – contact area; t – time; ΔP – difference in the partial pressures inside and outside the cups. The average of four measurements was taken as the result.

Antibacterial activity

The antibacterial activity against Gram-negative *Escherichia coli* (*E. coli* ATCC 25922) and Gram-positive *Staphylococcus aureus* (*S. aureus* ATCC 12600) was evaluated. Samples were sterilized at 121 psi prior to testing and immersed in a nutrient broth containing a 72-hour microbial culture at approximately 2.0×10^6 colony forming units/mL (CFU/mL). The samples were incubated for 24 h at 37°C, and the number of viable microbial colonies was counted manually using a counter-click and pen. These results were expressed as the average value of CFU/sample. All experiments were conducted without exposing the samples to the UV light. The survival ratio (SR) was estimated using the following formula:

$$SR = (N/N_o) \times 100 \quad (5)$$

N_o and N indicated the average number of bacterial colonies on pure EVA and nanocomposite films, respectively. The tests were carried out thrice and the average value was determined.

Nanocomposite films preparation

Prior to processing, EVA and ZnO were dried at 50ºC for 24 h. EVA was first melted at 160°C for 4 min, using an internal mixer (Plasticoder, Brabender), then ZnO (1, 3, and 5 wt%) was added and the process was continued for 6 min. The composites were pressed into 500 μm thick sheets using a compression moulding machine (GT-7014-H30C, GOTECH Co). The pressing temperature was 170°C, the preheating time was 4 min, and the pressing and the cooling time was 4 and 2 min, respectively. The samples were cut as required.

RESULTS AND DISCUSSION

Fourier transform infrared spectroscopy

FTIR analysis was performed to determine the effect of ZnO on the chemical structure of the EVA copolymer. The FTIR spectra show several absorption peaks related to the carboxylate impurities (Fig. 1). The peaks at 1630 and 1384 cm^{-1} are attributed to the asymmetric and symmetrical stretching of the zinc carboxylate, respectively, confirming the existence of reactive carbon-containing carboxylate moieties throughout the synthesis process [15]. The peaks at 2918, 2848 and 720 cm^{-1} are associated with $-CH_2$ bond of octadecylamine, and at 1466 cm-1 with stretching vibrations of the CN-amide bond [16]. However, after the addition of zinc oxide, the characteristic peaks of the EVA copolymer remained unchanged (Fig. 1), indicating a probable physical interaction between the oxide and the copolymer [17–19].

The carbonyl band can be used to assess the thermal degradation of the polymer matrix during processing. There were no additional carbonyl bands indicating EVA degradation and no increase in intensity and shift of the EVA acetate band at 1744 cm^{-1}, which proves that the copolymer chain did not break during processing [20, 21]. No changes in the intensity of carbonyl peaks were observed in the composites (Fig. 1). It can be concluded that the ZnO nanoparticles did not accelerate the degradation process and only physical interactions occurred between the polymer matrix and the filler [22, 23].

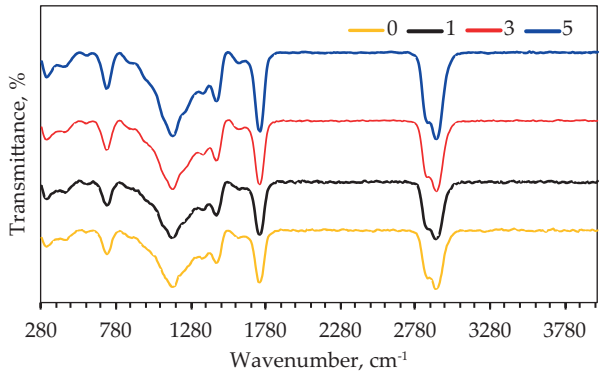

Fig. 1. Infrared spectra of pure EVA and EVA/ZnO nanocomposites

X-Ray diffraction analysis

Figure 2 shows the rhombic EVA structure with one peak at 2θ of 23°, which correspond to plane 200 [24, 25].

EVA crystallinity is controlled by the concentration of vinyl acetate, which is mainly related to the length of the ethylene segment [25–29]. The broad peak of the copolymer is related to the concentration of vinyl acetate, which ranges from 95 to 99% [22, 30]. The addition of zinc oxide nanoparticles increases the crystalline peak of EVA/ZnO composites, which suggests that zinc oxide improves the composite organization. The amorphous phase undergoes significant changes, showing that the zinc oxide causes crystal packing of the polymer chains, finally reducing the amorphous area. The change in nanoparticle content in the composite leads to higher copolymer crystallinity, which indicates an improvement in the structural organization of EVA after the oxide addition [31–33].

However, the oxide content higher than 3 wt% impairs the organization of the composite and causes the formation of zinc oxide peaks. The behavior of the EVA/ZnO (99/1) composite is comparable to that of pure polymer. An increase in the content of zinc oxide in the composite (Fig. 2) results in a decrease in the amorphous area, due to the increased influence of the matrix-modified zinc on the amorphous area, limiting the chain movement and increasing the polymer structural organization [16, 34]. The variation in EVA/ZnO composites performance, as well as the presence of the oxide peak in the diffraction pattern at the lowest ZnO content, indicate the limit concentration at which the matrix oxide dispersion fluctuates [35, 36].

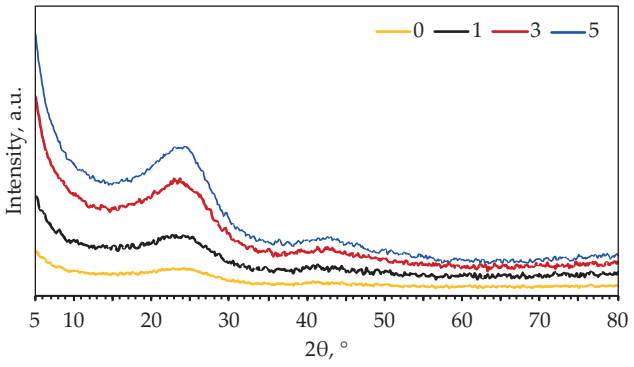

Fig. 2. XRD diffraction patterns of pure EVA and EVA/ZnO nanocomposites

Thermogravimetric analysis

The thermal decomposition of pure EVA and EVA/ZnO composites is shown in Figure 3. The TG curves of all samples show a one-step process of thermal degradation. The mass loss from 138°C to 384°C is due to the degradation of the olefin meres (C-C and C-H bonds). The addition of ZnO nanoparticles improves the thermal stability of EVA, as evidenced by the shift of the degradation temperature towards higher values (283–477°C) and the general tendency to increase thermal stability. The high thermal stability of the ZnO network, as well as the presence of connections between the nanoparticles and the polymer matrix, may be associated with the higher thermal stability [37–39].

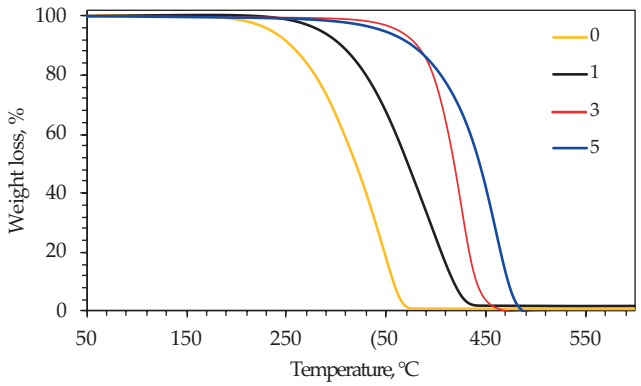

Fig. 3. TGA thermograms of pure EVA and EVA/ZnO nanocomposites

Water contact angle

The water contact angle **(**WCA) indicated the relative hydrophilicity and hydrophobicity of the substrates [3]. It referred to the angle between the substrate and a tangent line occurring at the contact point between the substrate and liquid droplet. This value defined the substrate wettability. A higher WCA indicates that the surface cannot be wetted easily and is therefore more hydrophobic [40]. Fig. 4 shows the contact angle of EVA/ZnO nanocomposites. Results revealed that the contact angle value of pure EVA (72° ± 2) was like those described in the literature [40]. The hydrophobicity of EVA/ZnO composites increased with increasing ZnO concentration. Addition of 1 and 3 wt% ZnO to EVA increased the number of polar groups in the composite, which was attributed to the presence of the polar ZnO. This further increased the surface energy of all composites, which slightly lowered WCA value compared to pure EVA. This common phenomenon was noticed when nanoparticles were incorporated into polymer composites. When the ZnO content increased to 5 wt%, there was a slight increase in the WCA value. However, the surface roughness of the composite increased significantly. As the surface roughness increased, the surface energy of the material decreased (i.e., the interfacial tension between the water and the polymer decreased), thereby increasing the hydrophobicity of the material (which was like the phenomenon observed in superhydrophobic materials). Polystyrene/

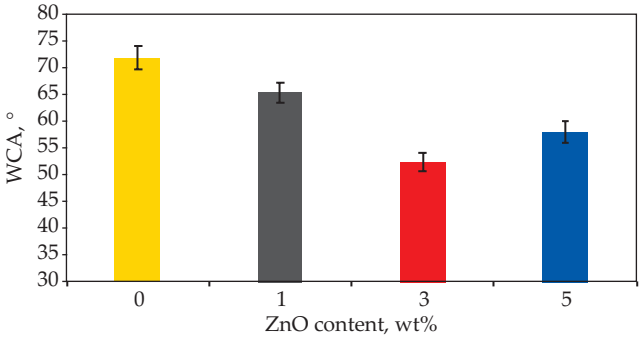

Fig. 4. Water contact angle for pure EVA and EVA/ZnO nanocomposites

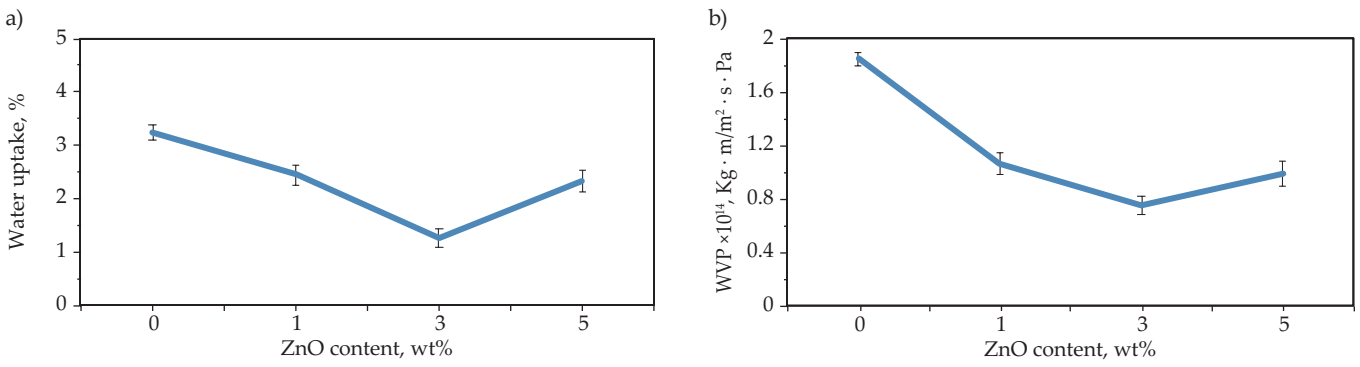

Fig. 5. Barrier properties of EVA/ZnO nanocomposite films: a) water uptake, b) WVP

ZnO composites showed similar behaviour [41]. Hence, a larger contact angle for the content of 5 wt% ZnO was attributed to surface roughness, despite the presence of polar ZnO particles (i.e., surface roughness was the dominant factor at higher ZnO content).

Barrier and swelling properties of the films

The main purpose of adding nanofillers to polymers is to obtain better barrier properties against vapours, gases, or other organic molecules of food packaging films. Excessive presence of moisture or oxygen is a major factor in accelerating food spoilage.

These permeants could easily get transported between the internal and external environments through the composite packaging walls, thereby causing a constant change in the shelf life and quality of the products. Hence, the particular barrier requirements were dependent on the characteristics of the products and their intended applications [42]. The results of water uptake and WVP are presented in Fig. 5. These parameters show a gradual decrease with an increase in the ZnO content. A minimal value of 46 and 69% was seen for these parameters, respectively, at the critical nanofiller load of 3wt%. Results highlighted the improvements noted for the barrier properties of the nanocomposite films against the water vapour and water compared to the pure polymer films. These improved values were higher than those noted for organoclay [43]. Furthermore, the increase in the ZnO loadings and crystallinity improved the tortuosity of the transportation path [44]. It was seen that this increase in the tortuosity level outweighed the increased hydrophilicity of the films. This finally decreased the water uptake and WVP of the films. For the nanocomposites with a higher ZnO loading, the decrease in these parameters was smaller than that noted in the sample with a 3 wt% content. This was attributed to the presence of small nanoparticle clusters that could form more preferred penetrant pathways, which could negatively affect the barrier performance.

Antibacterial properties of the films

Addition of different antibacterial compounds to the food packaging materials has garnered a lot of recent attention [45]. The nanocomposite antimicrobial systems were seen to be especially effective due to the higher surface to volume ratio along with a better surface reactivity of the nano-antimicrobial compounds. These properties of the nanocompounds helped them decrease the growth of the pathogenic microbes more effectively compared to the micro- or macrocompounds. The carbon nanotubes, metal nanoparticles (Ag, Cu, and Au) or metal oxide nanocompounds were generally used for developing antimicrobial agents. Though the silver ions have been generally used as an effective antimicrobial agent in the food and beverage storage-related applications, in the past few years, ZnO nanoparticles were seen to offer a safer and cost-effective packaging solution. Hence, in this study, the antibacterial activities of the EVA nanocomposite films against two human pathogenic microbes, i.e., *S. aureus* (gram-positive) and *E. coli* (gram-negative) were investigated. The results presented in Fig. 6 indicated that the survival ratio for both the microbes decreased significantly when the ZnO content increased. The highest antimicrobial activity was noted for the composite containing 3 wt% ZnO. The bacterial inactivation was investigated with respect to the homogenous dispersion of nanoparticles within the composites, which provided a large antimicrobial surface. The better bactericidal effect was observed for the nanocomposite with lower ZnO content, due to the better dispersion of nanoparticles in the polymer matrix, as discussed above. The efficiency of the antibacterial activity of the nanocomposites was influenced by numerous factors like the particle size distribution and their interaction with the polymer matrix [45]. For deriving the maximal effect of the antimicrobial properties of the nanoparticles, they must be homogeneously dispersed within the matrix without forming any aggregates. It was also seen that the antibacterial activity of the nanocomposites increased with a decrease in the par-

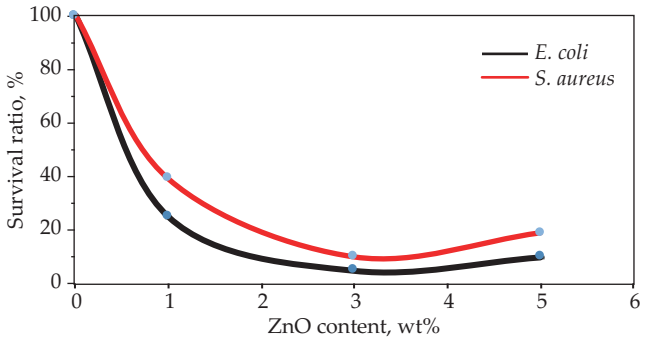

Fig. 6. Resistance of EVA/ZnO nanocomposites to survival of *E. coli* and *S. aureus*

ticle size [46]. Hence, the smaller clusters occurring in the composites containing 5 wt% ZnO behaved as large particles and exhibited a lower antibacterial activity compared to the individual nanoparticles.

CONCLUSIONS

The EVA-based nanocomposites reinforced with the uniformly dispersed ZnO nanoparticles were prepared by melt mixing, without using any additional coupling or surfactant molecules. The barrier, physical and antimicrobial properties were investigated. The nanocomposites exhibited antibacterial activity against the human pathogens. The antibacterial activity against *E. coli* was higher than against *S. aureus*. Optimum properties, i.e. maximum hydrophilicity with minimum water and WVP absorption, were obtained for the composite containing 3 wt% ZnO. The nanocomposites which displayed an antimicrobial activity could be used as effective alternatives to the synthetic stick-packaging materials, as they prevented the growth of pathogenic and food spoilage microbes. This increased the shelf life, safety, and quality of the food products during food storage and transportation.

REFERENCES

[1] Ding H., Fu TJ.: *Journal of Food Science* **2013**, *78*. https://doi.org/10.1111/1750-3841.12064
[2] Mihindukulasuriya SDF., Lim LT.: *Trends in Food Science and Technology* **2014**, *40*, 149. https://doi.org/10.1016/j.tifs.2014.09.009
[3] Rivero S., García MA., Pinotti A.: *Journal of Materials Physics and Chemistry* **2013**, *1*, 51. https://doi.org/10.12691/jmpc-1-3-5
[4] Peacock A.: https://www.taylorfrancis.com/books/mono/10.1201/9781482295467/ handbook-polyethylene-andrew-peacock (accessed 19 Jan **2023**).
[5] Reyes J.D.: *Celanese Corporation, TX, USA* **2014**, *1–6*.
[6] FINK JK.: (accessed 19 Jan **2023**).
[7] Marchante V., Benavente V., Marcilla A. *et al.*: *Journal of Applied Polymer Science* **2013**, *130*, *2987–2994*. https://doi.org/10.1002/app.39422
[8] Wilson R., Plivelic TS., Aprem AS. *et al.*: *Journal of Applied Polymer Science* **2012**, *123*, 3806–3818. https://doi.org/10.1002/app.34966
[9] George J., Bhowmick A.K.: *Journal of Applied Polymer Science* **2008**, *43*, 702. https://doi.org/10.1007/s10853-007-2193-6
[10] Gabriel M., Antônio J., Pierre B. *et al.*: *Journal of Applied Polymer Science B* **2011**, *1*. https://doi.org/10.17265/2161-6221/2011.09.016
[11] Lin H., Tzeng S., Hsiau P. *et al.*: *Nanostructured Mater* **1998**, *10*, 465. https://doi.org/10.1016/S0965-9773(98)00087-7
[12] Curri M., Comparelli R., Cozzoli P. *et al.*: *Materials Science and Engineering C* **2003**, *23*, 285. https://doi.org/10.1016/S0928-4931(02)00250-3
[13] Zhang L., Jiang Y., Ding Y. *et al.*: *Journal of Nanoparticle Research* **2007**, *9*, 479. https://doi.org/10.1007/s11051-006-9150-1
[14] Oh J., Lim S., Ahn S. *et al.*: *Journal of Physics D* **2013**, *46*. https://doi.org/10.1088/0022-3727/46/28/285101.
[15] Hameed K., Salmiaton A., Mohamad H. *et al.*: *Bulletin of Chemical Reaction Engineering and Catalysis* **2017**, *12*, 81.
[16] Albalushi M.Y., Abdulkreem-Alsultan G., Asikin-Mijan N. *et al.*: *Catalysts* **2022**, *12*, 1537.
[17] Alsultan A.G., Asikin Mijan N., Mansir N. *et al.*: *ACS Omega* **2021**, *6*, 408.
[18] Aziz N., Yunus R., Hamid H. *et al.*: *Sci Rep* **2020**, *10*, *1*.
[19] Alsultan A.G., Asikin-Mijan N., Ibrahim Z. *et al.*: *Catalysts* **2021**, *11*, 1261.
[20] Abdulkareem-Alsultan G., Asikin-Mijan N., Taufiq-Yap YH.: *Engineering Materials* **2016**, 75.
[21] Abdulkareem Ghassan A., Mijan N., Hin Taufiq-Yap Y.: *Nanorods and Nanocomposites* **2020.** https://doi.org/10.5772/intechopen.84550
[22] Shobhana G., Asikin-Mijan N., AbdulKareem-Alsultan G. *et al.*: *Biomass and Bioenergy* **2020**, *141*, 105714.
[23] Abdulkareem-Alsultan G., Asikin-Mijan N., Lee H.V. *et al.*: *Innovations in Sustainable Energy and Cleaner Environment. Green Energy and Technology*. Springer Singapore **2020**, pp 489–504.
[24] Albazzaz A. S., GhassanAlsultan A., Ali S. *et al.*: *Journal of Energy, Environmental and Chemical Engineering* **2018**, *3(3)*, 40.
[25] Lim S.T., Sethupathi S., Alsultan A.G. *et al.*: *Energy and Fuels* **2021**, *35*, 16212.
[26] Abdulkareem-Alsultan G., Asikin-Mijan N., Obeas L.K. *et al.*: *Chemical Engineering Journal* **2022**, *429*, 132206.
[27] Asikin-Mijan N., Sidek H.M., Alsultan A.G. *et al.*: *Catalysts* **2021**, *11*. https://doi.org/10.3390/catal11121470
[28] Shah I., Adnan R., Alsultan A.G. *et al.*: *Journal of Dispersion Science and Technology* **2020**, *0*, 1–16.

[29] Alsultan A., Asikin-Mijan N., Obeas L. *et al*.: *Catalysts* **2022**, *12,* 566.
[30] Mansir N., Mohd Sidek H., Teo S.H. *et al*.: *Bioresource Technology Reports* 2022, *17,* 100988.
[31] Adzahar N.A., Asikin-Mijan N., Saiman M.I. *et al*.: *RSC Advances* **2022**, *12,* 16903.
[32] Alsultan A.G., Mijan N. A., Mastuli M.S *et al.: Fuel* **2022**, 325, *124917.*
[33] Wondi M.H., Shamsudin R., Yunus R. *et al*.: *Journal of Food Process Engineering* **2020**, *43,* doi:10.1111/jfpe.13426.
[34] Abdulkareem-Alsultan G., Asikin-Mijan N., Taufiq-Yap Y.H.: *Green Energy and Technology*. Springer Science and Business Media Deutschland GmbH **2021**, pp 505–522.
[35] Ravindran M.X.Y., Asikin-Mijan N., Ong H.C. *et al*.: *Journal of Analytical and Applied Pyrolysis* **2022**, *168*. https://doi.org/10.1016/j.jaap.2022.105772
[36] Razali S. Z., Yunus R., Kania D. *et al*.: *Journal of Materials Research and Technology* **2022**, *21,* 2891.
[37] Abdulkareem-Alsultan G., Asikin-Mijan N., Kareem O.L. *et al*.: *Product Technology Prop App* **2023**, doi:10.5772/intechopen.104984.
[38] Asikin-Mijan N., Derawi D., Salih N. *et al*.: *Innovations in Thermochemical Technologies for Biofuel Processing* **2022**, 197.
[39] Abdulkareem-Alsultan G., Asikin-Mijan N., Lee H.V. *et al*.: *Catalysts* **2019**, *9,* 1.
[40] Shafrin E.G., Zisman W.A.: *The Journal of Physical Chemistry A* **1960**, *64,* 519. https://doi.org/10.1021/j100834a002
[41] Qing Y., Zheng Y., Hu C. *et al*.: *Applied Surface Science* **2013**, *285,* 583. https://doi.org/10.1016/j.apsusc.2013.08.097
[42] Siracusa V., Rocculi P., Romani S. *et al*.: *Trends in Food Science and Technology* **2008**, *19, 634*. https://doi.org/10.1016/j.tifs.2008.07.003
[43] Shafiee M., Ramazani S.A.: *Macromolecular Symposia* **2008**, *274*, 1. https://doi.org/10.1002/masy.200851401
[44] Alakrach A.M, Noriman N.Z, Dahham O.S. *et al*.: *IOP Conference Series: Materials Science and Engineering* **2019**, *557.* https://doi.org/10.1088/1757-899X/557/1/012067
[45] Laycock B., Halley P., Pratt S. *et al*.: *Progress in Polymer Science* **2014**, *39, 397.* https://doi.org/10.1016/j.progpolymsci.2013.06.008
[46] Tam K.H., Djurišić A.B., Chan C.M.N. *et al*.: *Thin Solid Films* **2008**, *516,* 6167. https://doi.org/10.1016/j.tsf.2007.11.081

Received 25 I 2023.